AJR FOCUS ON:

Value-Added Opportunistic CT: Insights Into Osteoporosis and Sarcopenia

Robert D. Boutin[1]
Leon Lenchik[2]

OBJECTIVE. The purpose of this article is to review the emerging field of opportunistic CT, which can be used to screen patients for osteoporosis and sarcopenia.

CONCLUSION. Although body composition measurements are not routinely obtained using CT, quantitative assessment of bone and muscle biomarkers on CT can add value to patient care. Automated bone and muscle measurements promise to transform the everyday practice of radiology without resulting in additional cost or radiation exposure for patients.

Just 100 years ago, our planet's population was less than one-quarter its current size [1], the mean life span was 35 years [2], and communicable diseases were the leading cause of death [3]. Now the population exceeds 7.7 billion people (with that number increasing by more than 200,000 every day) [4], the mean life expectancy worldwide is more than 73 years [4], and noncommunicable diseases are the leading cause of death among older adults [3].

The doubling of the population older than 60 years of age worldwide during the next three decades [4] is expected to bring with it a tsunami of age-related conditions and an increased demand for imaging services for a growing middle class. In the United States, health care costs continue to rise at a seemingly unsustainable rate [5] (such costs now represent approximately 18% of the gross domestic product [6]), with spending on medical imaging estimated to be $100 billion per year [7]. Because of these intensifying fiscal pressures and calls to curb wasteful diagnostic imaging [8], payment rates for imaging are projected to decrease [9] unless added value can be shown.

In the setting of this looming health care crisis, there is an urgent need to implement new approaches to add value to imaging. One such approach is to derive new biomarkers from routine imaging examinations. This is commonly referred to as opportunistic imaging.

The purpose of the present article is to review the highlights of opportunistic imaging by focusing on the use of opportunistic CT to screen for osteoporosis and sarcopenia. After discussing the current use of CT for opportunistic imaging of musculoskeletal tissues, we review the technical considerations in obtaining accurate CT measurements of bone and muscle and provide a rationale for obtaining body composition measurements to help improve clinical outcomes.

Opportunistic Imaging: Why CT?

Although opportunistic imaging can be performed using any imaging modality, CT has been the most extensively studied modality for three reasons. First, CT is a very common imaging technique. In the United States, for example, more than 88 million CT scans were obtained in 2018, compared with 39 million MRI scans (i.e., 245 vs 118 scans, respectively, per 1000 people) [10]). Second, CT is a first-line cross-sectional imaging technique for evaluating many acute and chronic disorders associated with aging, including fractures, frailty, cancer, and cardiometabolic syndrome [11]. Third, CT measurements of many tissues are relatively easy to obtain, are highly reproducible, and have been associated with many important clinical outcomes, including death [12, 13].

Opportunistic CT: What Tissues?

In theory, opportunistic CT can be used to obtain quantitative biomarker data from any tissue included in a routine imaging evaluation. In practice, however, CT is used most commonly to evaluate tissues that provide practical insights into the biologic age of a patient. Indeed, characterizing biologic age

Keywords: CT, muscle, musculoskeletal, osteoporosis, sarcopenia

doi.org/10.2214/AJR.20.22874

Received January 25, 2020; accepted after revision February 24, 2020.

Based on a presentation at the Radiological Society of North America 2019 annual meeting, Chicago, IL.

Supported by grant P30 AG021332 from the National Institutes of Health Pepper Center.

[1]Department of Radiology, Stanford University School of Medicine, 300 Pasteur Dr, MC-5105, Stanford, CA 94305. Address correspondence to R. D. Boutin (boutin@stanford.edu).

[2]Department of Radiology, Wake Forest School of Medicine, Winston-Salem, NC 27157.

AJR 2020; 215:582–594

ISSN-L 0361–803X/20/2153–582

(rather than relying on chronologic age) furthers the goal of precision medicine in which the characteristics (phenotypes and genotypes) of a specific individual replace the previously accepted medical standard of caring for a typical patient. This approach aims to improve risk stratification so that finite health care resources, including the prescription of specific prevention and treatment regimens, can be deployed more optimally.

Various tissues that have been investigated using CT are beyond the scope of this article; these include quantitative biomarkers associated with vasculature (e.g., aortic and coronary artery calcification scoring for atherosclerosis) [14, 15], fat (e.g., size and attenuation for adiposity) [16], liver (e.g., fat quantification for steatosis) [17], and hepatosplenic morphologic features (e.g., volumetric assessment for staging liver fibrosis) [18].

In the musculoskeletal system, the most widely studied biomarkers are in bone (e.g., attenuation for osteoporosis) and muscle (e.g., size and attenuation for sarcopenia). Each individual biomarker may have merit as an independent predictor of particular clinical outcomes. Together, a synergistic combination of these biomarkers could potentially provide even more prognostic power for personalized risk stratification.

Regardless of the tissue assessed, many technical factors can influence measurement accuracy and reproducibility (precision), resulting in important implications for clinical utility.

Technical Considerations

CT measurements can be influenced by variations in patient factors, CT protocols, and measurement methods, even if scanners are properly calibrated. The potential for methodologic errors highlights the importance of protocol standardization (or empirical corrections) when analyzing body composition. Although these parameters often are not reported in published studies of opportunistic CT results, it is recommended that future publications account for relevant variables [19, 20].

Patient Factors

For measuring bone and muscle, both patient diameter and the positioning of body parts within the scanner are important considerations.

Patient diameter—Patient diameter can vary considerably (e.g., in patients with cachexia vs obesity). With increasing diameters, attenuation measurements (both mean and SD values) can increase by approximately 5–7 HU, regardless of the tube potential used (Boutin RD, et al., presented at the National Cancer Institute 2017 workshop Understanding the Role of Muscle and Body Composition). Furthermore, with greater object size, lower-energy photons are more heavily attenuated than higher-energy photons, the effective energy seen by the CT detectors is higher, and there is a spurious change in attenuation values from the periphery to the center of the object.

Patient positioning—CT number measurements should be interpreted with caution when patients are positioned off-center in a scanner. Clinically realistic off-centering (approximately 6 cm above or below isocenter) can result in a spurious increase of more than 20 HU in the CT number obtained using scanners with a traditional bowtie filter with filtered back projection [21]. Newer model-based iterative reconstruction algorithms [22] and dual-energy techniques [23] may be less susceptible to inaccuracies associated with patient positioning.

CT Technique

For bone and muscle measurements, the two most important factors that influence CT numbers are IV contrast material and tube potential. Other factors include tube current [24], slice thickness [24, 25], reconstruction kernel [26], and the type of CT scanner used [26–28].

Contrast material—Accounting for IV contrast material on CT measurements is challenging because of inconsistencies in tissue characteristics, bolus timing, contrast volume, contrast concentration, contrast injection rate, cardiac output, and beam-hardening artifact [29].

With measurements of trabecular bone in the lumbar spine, for example, vertebral body enhancement varies from a mean of approximately 17 HU in the arterial phase to 33 HU in the portal phase, to 25 HU in the delayed phase [20] (Fig. 1). Contrast enhancement in the lumbar spine has been reported to be as low as 10–26 HU in previous studies [30, 31]. Consequently, if bone measurements are not adjusted for contrast enhancement, contrast-enhanced CT can result in underdiagnosis of osteoporosis in 7–25% of patients [30].

Elsewhere in the skeleton, data on contrast-enhanced attenuation are less definitive, but variations are known to occur. For example, although contrast-enhanced quantitative CT measurement of bone mineral density (BMD) in the spine increases 30% [32] or 31% [33], BMD increases only 2% in the proximal femur [33].

With skeletal muscle, the magnitude of change in muscle attenuation related to IV contrast medium ranges from approximately 5 HU (in the arterial phase) to approximately 11.5 HU (in the portal phase), to approximately 13 HU (in the delayed phase) at the L4 level [20]. When tube potential is held constant, such changes in contrast-enhancement can result in an approximately 2–3% increase in muscle metric measurements [24,

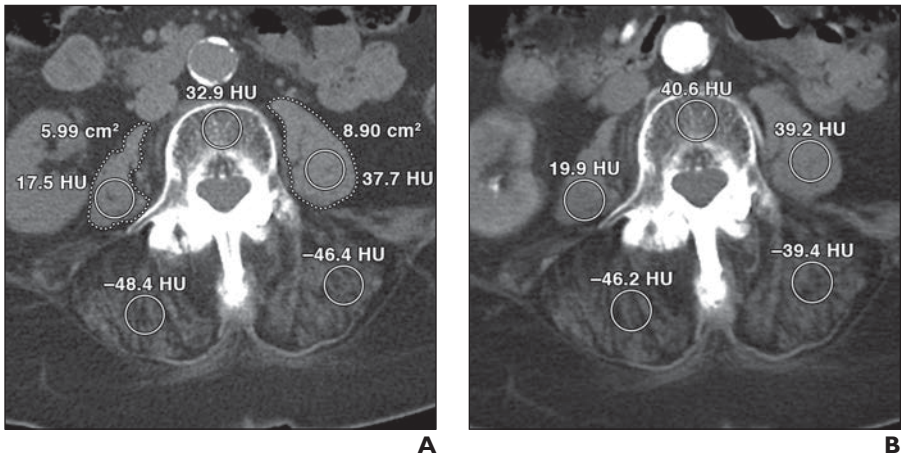

Fig. 1—88-year-old woman with right upper quadrant and back pain. (Reprinted from [20])
A–D, Representative four-phase CT scans obtained in unenhanced phase (**A**), arterial phase (**B**), portal phase (**C**), and delayed phase (**D**) show ROIs (*circles*) for psoas muscles, posterior paraspinal muscles, and L4 vertebral body. For example, attenuation of L4 vertebral body increased from 32.9 HU in unenhanced phase to 40.6 HU in arterial phase, 50.3 HU in portal phase, and 59.5 HU in delayed phase. Attenuation of abdominal aorta also was measured on each of four phases of CT examination at L3 level above level of aortic bifurcation (not shown). In **A**, dotted lines show freehand ROIs drawn on unenhanced images outlining both psoas muscles.

(Fig. 1 continues on next page)

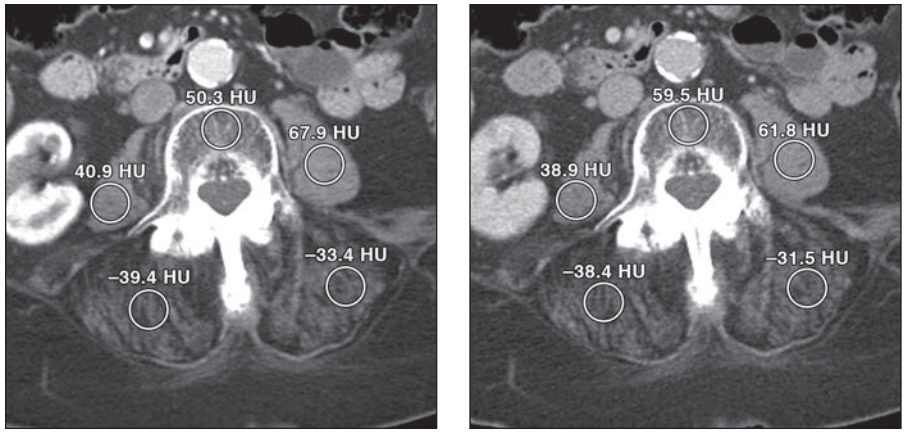

C D

Fig. 1 (continued)—88-year-old woman with right upper quadrant and back pain. (Reprinted from [20])
A–**D**, Representative four-phase CT scans obtained in unenhanced phase (**A**), arterial phase (**B**), portal phase (**C**), and delayed phase (**D**) show ROIs (*circles*) for psoas muscles, posterior paraspinal muscles, and L4 vertebral body. For example, attenuation of L4 vertebral body increased from 32.9 HU in unenhanced phase to 40.6 HU in arterial phase, 50.3 HU in portal phase, and 59.5 HU in delayed phase. Attenuation of abdominal aorta also was measured on each of four phases of CT examination at L3 level above level of aortic bifurcation (not shown). In **A**, dotted lines show freehand ROIs drawn on unenhanced images outlining both psoas muscles.

25], but small changes in muscle size are not likely to be clinically significant [34, 35]. Core muscles affected by myosteatosis (as indicated by attenuation of < 30 HU) can be particularly vulnerable to changes in contrast enhancement, with the size of these areas of fat within muscle found to be a mean of 14% smaller than the size of such areas as seen on unenhanced series [25].

Tube potential—Tube potential can substantially influence CT number measurements, especially those for bone [36]. As tube potential decreases, the CT number increases, especially for tissues with higher electron attenuation values. Specifically, with trabecular bone measurements, an increase of 60 kV (from 80 to 140 kV) can result in a change of –76 HU [36]. Although 120 kV is a common standard, conversion equations may be used for scans acquired at other settings (e.g., CT myelography performed at 140 kV [37]).

For soft tissues such as muscle, changes in tube potential do not result in such large changes in CT numbers on unenhanced scans. However, the iodine in contrast material results in increased attenuation at 80 kV compared with 140 kV, and this can cause misclassification of tissues with substantial uptake of contrast medium, including muscle [38].

Measurement Methods

Software tools—Software used for analysis of body composition may result in modest variability in bone and muscle measurements [39], but common commercially available software programs generally produce comparable results with good interobserver and intraobserver agreement [39–41]. CT-derived bone and muscle metrics have been associated with clinical outcomes in a variety of different studies, regardless of whether the measurements were made using a routine PACS ROI tool (without postprocessing) or with postprocessing using a thresholding step for tissue segmentation (e.g., ImageJ, [National Institutes of Health]; OsiriX [Pixmeo], or SliceOmatic [TomoVision]).

Manual measurements—When manual measurements of CT numbers are obtained using a single software platform, the interexamination, interobserver, and intraobserver results vary from moderate to excellent [24, 35, 42]. With low-dose unenhanced chest CT, for example, manual measurements of L1 attenuation have an excellent interexamination agreement (interclass correlation coefficient, 0.92) and moderate-to-excellent interobserver agreement (interclass correlation coefficient, 0.70–0.91) [42]. One study [42] indicated that a change of at least 28 HU is needed to detect a real change in bone attenuation between examinations and that there can be discordance of 12 HU in measurements of bone attenuation made by individual observers. Such interexamination and interobserver results of low-dose CT can lead to reclassification of osteoporosis for 11% and 22% of patients, respectively [42].

Automated algorithms—Automated algorithms can produce substantial variations in results caused by differences in slice selection or ROI placement. For example, in comparisons of manual versus fully automated measurements obtained at the L1 vertebral body, the fully automated algorithm resulted in measurements that were a mean of 21 HU higher than manual measurements [43]. This difference may have been the result of off-midline measurements and highlights the need for rigorous validation of automated algorithms. In general, however, machine learning algorithms compare favorably to manual measurements of bone and muscle [43–46].

Osteoporosis

Osteoporosis, which is defined by the presence of low bone mass and quality, results in increased bone fragility and fracture risk. Major osteoporotic fractures and, possibly, low BMD by itself may be associated with premature death [47]. Between 2018 and 2040 in the United States, the incidence of osteoporotic fractures is projected to increase 68% (from 1.9 to 3.2 million annually) [48].

Although there is a high general awareness of osteoporosis among patients and health care providers, there are large gaps in both the diagnosis and treatment of osteoporosis [49, 50]. In the United States, for example, improved diagnosis and treatment of osteoporosis could prevent more than 6 million fractures and save $83 billion over the next 22 years [48]. Despite the proven efficacy of dual-energy x-ray absorptiometry (DEXA) screening for reduction of fracture risk [51], DEXA utilization has actually declined in the United States [52], with underutilization and undertreatment noted even after a sentinel fracture [53, 54]. Given that fewer than 6% of older women (age > 65 years) who have undergone CT of the chest or abdomen have undergone a DEXA examination (Raulli AO, et al., presented at the Radiological Society of North America 2019 annual meeting), opportunistic CT could help bridge the existing gap in osteoporosis screening.

Methodology

Traditional bone mineral density approach—The traditional approach to quantitative CT calculates volumetric BMD (measured as milligrams per cubic centimeters) by using specialized software and a specialized BMD calibration phantom. The specialized phantom can be placed under the patient (known as synchronous external calibration) [55] or scanned at a different time than the patient is scanned (known as synchronous external calibration) [56]. CliniQCT (Mindways Software)

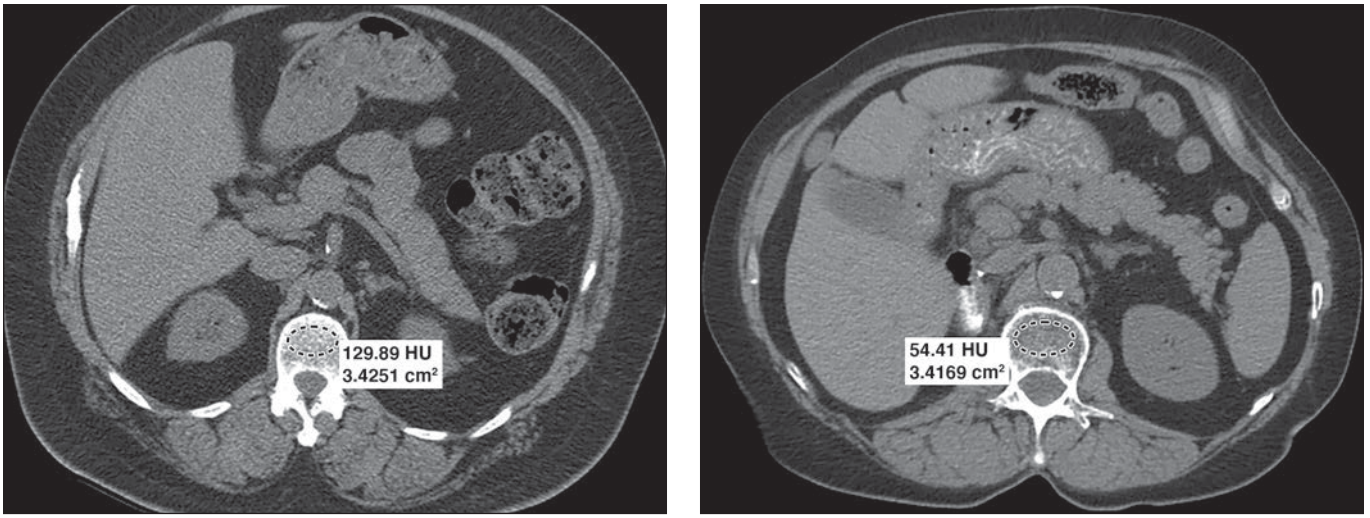

Fig. 2—Images from opportunistic CT of bone. Dashed ovals denote ROIs.
A, 68-year-old woman who presented with possible renal calculus. Axial CT image obtained at level of L1 shows mean vertebral trabecular attenuation of 129.89 HU. Using diagnostic threshold of 90 HU, opportunistic CT measurement is within range considered normal.
B, 75-year-old woman who presented with abdominal pain. Axial CT image obtained at level of L1 shows mean vertebral trabecular attenuation of 54.41 HU. Using diagnostic threshold of 90 HU, opportunistic CT measurement is within range indicating osteoporosis.

is a commercially available product that uses the latter approach. An alternative phantomless approach calibrates attenuation measurements by use of adjacent internal tissue (e.g., blood, muscle, and fat) and air. VirtuOst software (O.N. Diagnostics) is a commercially available product that uses this approach. Although these techniques are powerful research tools, they have not yet gained widespread acceptance as clinical tools for osteoporosis screening.

New approach to attenuation measurement—Direct measurements of trabecular bone attenuation are increasingly used for osteoporosis screening in clinical research and practice. Reliable results depend on careful attention to standard operating procedures, including quality assurance programs (e.g., daily asynchronous calibration using an American College of Radiology phantom). Opportunistic screening for osteoporosis is a dynamic area of research because measurement of bone attenuation is easy to perform on any workstation with standard viewing software. Window settings do not affect the attenuation values, but bone windows are recommended to facilitate appropriate ROI selection. The imaging plane generally has only a minimal influence on attenuation values [57].

In the spine, the ROI is placed on the vertebral body trabecular bone, avoiding the venous plexus posteriorly (Fig. 2). The L1 vertebra is measured most commonly because it is generally included on CT examinations of the thoracolumbar spine, chest, and abdomen. If L1 cannot be measured (e.g., because of a compression fracture, hemangioma, bone island, or artifact), then an adjacent level (e.g., T12 or L2) can be measured (Fig. 3). Among the lumbar levels, bone attenuation tends to be lowest at L3, with slightly higher mean attenuation seen at more proximal and distal levels [58]. Of importance, the mean attenuation values for trabecular bone are generally very similar from T12 to L5 [58].

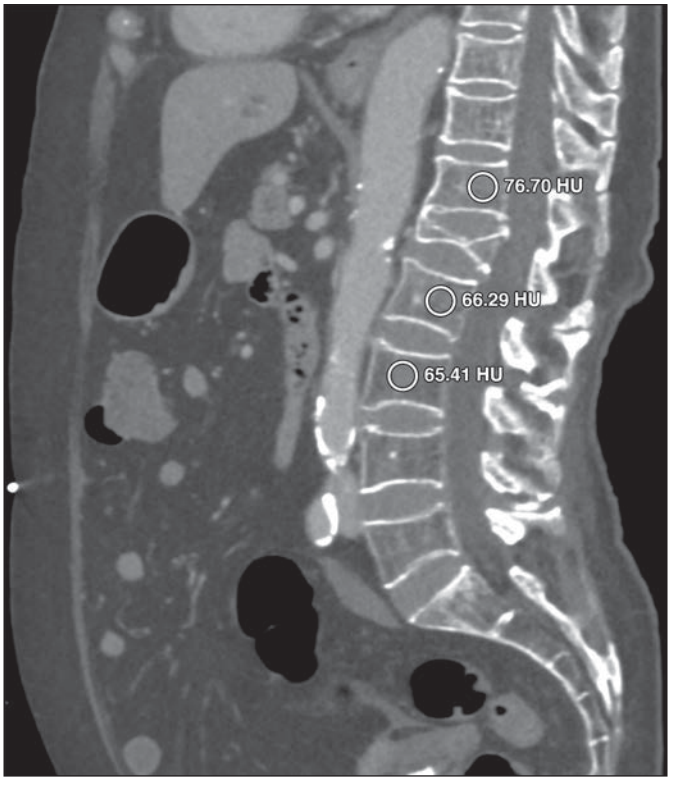

Fig. 3—67-year-old woman who presented to emergency department with abdominal pain. Sagittal CT image allows efficient assessment of both nonacute L1 vertebral body fracture and measurement of mean bone attenuation at adjacent levels (avoiding fractured L1 level and foci of osteosclerosis in T12 and L2 vertebral bodies). Note that level with lowest mean attenuation is L3 (65.41 HU). Using diagnostic threshold of 90 HU, opportunistic CT measurement is within range indicating osteoporosis. Circles denote ROIs.

Clinical Applications

Lumbar spine—Direct attenuation measurements of bone have been used in many recent studies (Appendix 1), most commonly at the L1 level. Much of the seminal work has been performed by investigators at the University of Wisconsin who established that the attenuation values of bone correlate with DEXA-derived BMD and predict fracture outcomes, and these investigators first used the term "opportunistic CT" in their 2011 study [59].

Specific thresholds have been suggested for identifying or ruling out osteoporosis at the L1 level. Osteoporosis is generally present at an attenuation of 90 HU or less (specificity, > 90%); this cut point also is associated with prevalent vertebral fractures (odds ratio, 32) and incident fragility fractures throughout the skeleton [60, 61]. The prevalence of fracture tends to have an inverse association with attenuation values; the prevalence of vertebral fracture increases to almost 50% when the attenuation at L1 is 50 HU or less [60]. Conversely, attenuation of more than 160 HU essentially rules out osteoporosis, with a negative predicative value of 95%.

In addition to reviewing sagittal CT images for compression fractures [62], it is increasingly common to measure L1 attenuation and report values of less than 100 HU as indicating likely osteoporosis. Correlation with DEXA findings is currently recommended for these patients. In the future, the role of DEXA as the reference standard may diminish as clinicians become more comfortable with CT results and new evidence emerges to indicate that opportunistic CT can predict vertebral fractures better than DEXA [63].

One of the obstacles to closing the gap in osteoporosis treatment is that some referring providers are not comfortable with osteoporosis management. To address this, many institutions have specialists (e.g., a fracture liaison service) who are committed to evidence-based osteoporosis care. For any provider involved in osteoporosis care, the following information is particularly important: first, most vertebral fractures are clinically occult but are associated with a high risk of future fractures, including hip fractures; second, the proportion of patients starting antiosteoporosis medication within a year after a vertebral compression fracture is low (< 30%) [53, 54]. For these reasons, providers who care for patients at risk for osteoporosis and associated fractures should be more proactive in their diagnosis and treatment to reduce the burden of future fractures [53, 54].

One group of specialists that has shown particular interest in this field is spine surgeons. Recent retrospective studies suggest that low attenuation values correlate with poor surgical outcomes, including pedicle screw loosening [37, 64], cage subsidence [65], nonunion after a lumbar interbody fusion procedure [66], and postoperative fracture involving an adjacent level resulting in proximal junctional kyphosis [67].

Although further studies are needed, some authors recommend use of a threshold of less than 120 HU in the lumbar spine to indicate an increased risk of screw loosening, cage subsidence, and interbody fusion pseudarthrosis [68]. For patients with lumbar spine attenuation of less than 120 HU who undergo lumbar or thoracic fusion with pedicle screws, screw augmentation has been suggested [64]. When lumbar spine attenuation values of less than 50 HU are present, even screw fixation with bone cement augmentation is associated with poor outcomes [69]. Risk stratification using CT may aid patients and surgeons in making informed decisions about the need for antiosteoporosis medications and the timing of an elective spine surgery.

In the past, there was concern that bisphosphonate treatment might impair successful fusion after a spine fusion procedure. It is now recognized that bisphosphonates do not impair successful osseous fusion [70] and that they in fact reduce the risk of postoperative cage subsidence [70, 71] and vertebral fracture [70].

Beyond the lumbar spine—Various bones have been studied less extensively than the lumbar vertebrae [72]. CT studies of the appendicular skeleton generally assess mean attenuation for a representative area of trabecular bone and indicate that attenuation values are highly correlated with BMD measurements made by DEXA.

Extraspinal opportunistic CT studies have evaluated the frontal bone [73], shoulder [74], wrist [75], sacrum [76], hip [77, 78], knee [78, 79], ankle [78], and foot [80]. Although they need further validation, provisional thresholds for diagnosing osteoporosis have been proposed for the proximal humerus (92 HU) [74], distal radius (231 HU) [75], femoral head (296 HU) [78], mid femoral neck (262 HU) [77], distal tibia (122 HU) [78], and talus (311 HU) [78]. Given that patients with osteoporotic bone are predisposed to hardware complications (e.g., implant cut out, implant loosening, and periimplant fracture), there is intense interest in proactively identifying bones with osteoporosis that may benefit from personalized modifications (e.g., supplemental hardware, augmentation with calcium phosphate or polymethylmethacrylate, interlocking lag screws, or angle-stable locking plates) [81].

Currently, the cutpoints at these sites are not universally accepted for the diagnosis and treatment of osteoporosis, for at least three reasons. First, the appendicular skeleton is scanned less frequently than the axial skeleton. Second, osteoporotic fractures are most common in the spine. Finally, although the trabecular pattern in thoracolumbar vertebrae is relatively uniform, many other bones have variable trabecular architecture that makes consistent attenuation measurements more challenging. In the sacrum, for example, large regional differences in attenuation measurements have been reported between the S1 body (224 HU), lateral sacral ala (100 HU), and central ala (24 HU) in a population of patients with a mean L1 attenuation of 165 HU [76].

Sarcopenia

Definition

Sarcopenia is broadly defined by the loss of muscle mass and muscle function. In clinical practice and clinical research, sarcopenia has been defined by expert consensus panels including the European Working Group on Sarcopenia in Older People, the Asian Working Group for Sarcopenia, the International Working Group on Sarcopenia, the Foundation for the National Institutes of Health Sarcopenia Project, and the Sarcopenia Definitions and Outcomes Consortium supported by the Foundation for the National Institutes of Health Sarcopenia Project. These definitions rely on measurements of physical function that include slow walking speed (e.g., ≤ 0.8 m/s) and low grip strength (e.g., < 27 kg for men and < 16 kg for woman) [82]. Among older adults, both slow gait and weak grip are established risk factors for disability and mortality.

Since the publication of an earlier in-depth review of sarcopenia in the *AJR* [83], the term "acute sarcopenia" has entered the lexicon to refer to accelerated muscle depletion that can occur with events such as surgery, hospitalization, and chemotherapy. In addition, DEXA-derived appendicular lean mass has fallen out of favor as one of the primary metrics in the diagnosis of sarcopenia, on the basis of analysis of more than 18,000

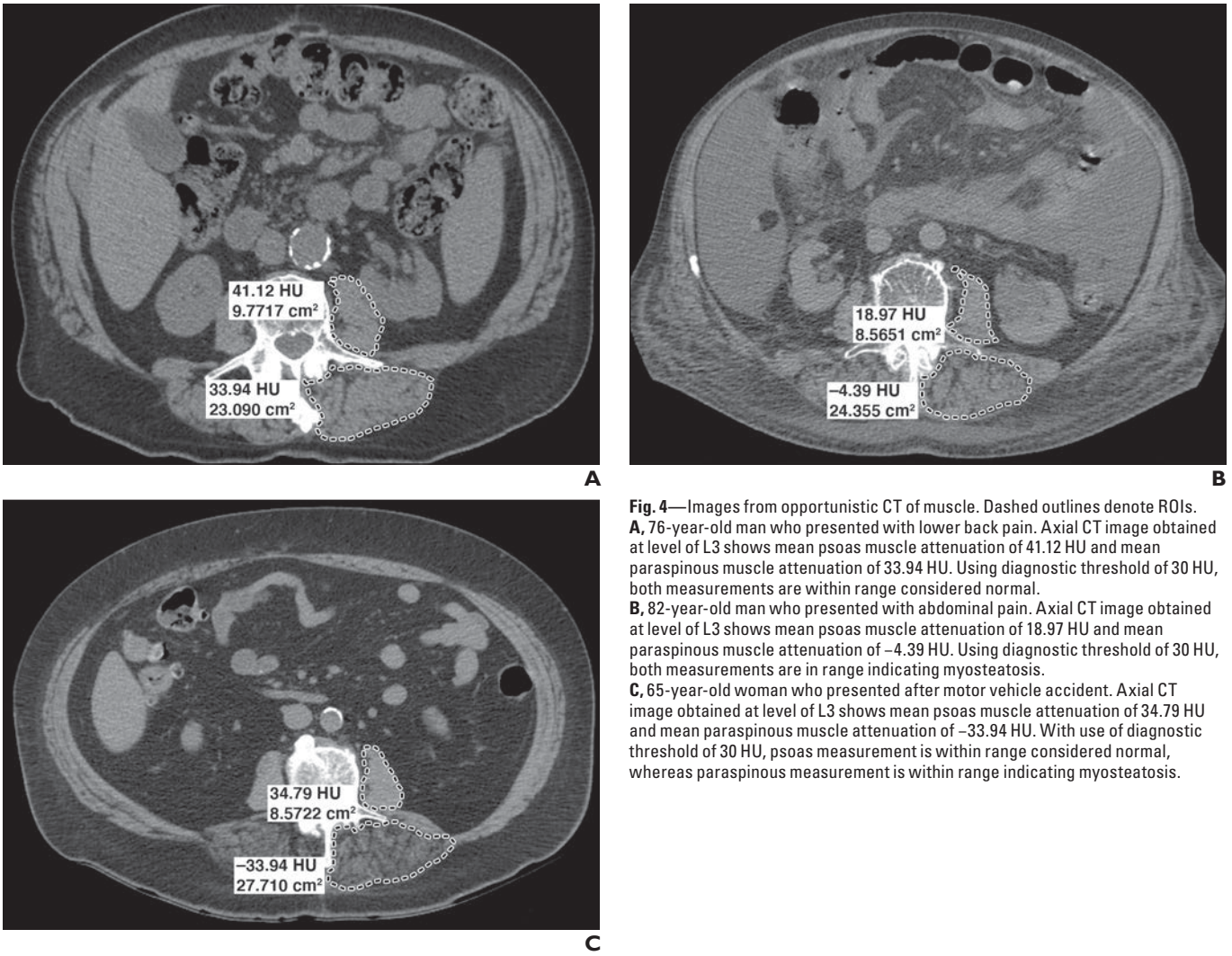

Fig. 4—Images from opportunistic CT of muscle. Dashed outlines denote ROIs.
A, 76-year-old man who presented with lower back pain. Axial CT image obtained at level of L3 shows mean psoas muscle attenuation of 41.12 HU and mean paraspinous muscle attenuation of 33.94 HU. Using diagnostic threshold of 30 HU, both measurements are within range considered normal.
B, 82-year-old man who presented with abdominal pain. Axial CT image obtained at level of L3 shows mean psoas muscle attenuation of 18.97 HU and mean paraspinous muscle attenuation of –4.39 HU. Using diagnostic threshold of 30 HU, both measurements are in range indicating myosteatosis.
C, 65-year-old woman who presented after motor vehicle accident. Axial CT image obtained at level of L3 shows mean psoas muscle attenuation of 34.79 HU and mean paraspinous muscle attenuation of –33.94 HU. With use of diagnostic threshold of 30 HU, psoas measurement is within range considered normal, whereas paraspinous measurement is within range indicating myosteatosis.

research subjects by the Sarcopenia Definitions and Outcomes Consortium [84].

Although the diagnostic criteria for various consensus definitions are similar, the small differences that do exist may result in substantial inconsistency in the clinical diagnosis of sarcopenia [85–88].

Prevalence

The prevalence of sarcopenia generally increases with advancing age and comorbidities. In a recent systematic review of almost 35,000 participants worldwide, the prevalence was lowest among community-dwelling adults (11% for men and 9% for women), more common among hospitalized patients (23% for men and 24% for women), and most common among nursing home residents (51% for men and 31% for women) [89].

With respect to comorbidities in the general population, a recent study of more than 17,000 individuals with age-associated diseases and more than 22,000 control individuals without such diseases found that sarcopenia was most prevalent in individuals with cardiovascular disease (31%), diabetes mellitus (31%), respiratory disease (27%), and dementia (26%) [90]. Emerging data indicate that the risks of cognitive impairment are more than doubled for patients with sarcopenia (compared with those without sarcopenia) [91]. These studies of age-associated comorbidities with sarcopenia suggest that the value of opportunistic imaging in clinical practice will increase for many years to come.

Opportunistic CT Diagnosis and Outcomes

In addition to inconsistencies in the clinical criteria for diagnosis of sarcopenia, the CT criteria used to diagnose sarcopenia have also been highly varied [19, 92]. In 388 CT studies in a recent systematic review [19], the most commonly used technique was to assess all skeletal muscle on an axial slice at the L3 vertebral level. Muscle measurement techniques have been studied both with a routine PACS ROI tool (without postprocessing) (Fig. 4) and with postprocessing that uses a thresholding step for tissue segmentation [12, 13, 83] (Fig. 5). In addition to the L3 level, many other anatomic sites have been reported, including the psoas muscle at the L4 level, the posterior paravertebral musculature at the T12 level (Fig. 6), and the thigh musculature [83] (Fig. 7).

At each location, CT is typically used to evaluate muscle size and attenuation. CT assessment of muscle size usually involves measuring muscle cross-sectional area (expressed as square centimeters) on an axial CT image, often with an adjustment for patient height (expressed as square meters), resulting in a skeletal muscle index.

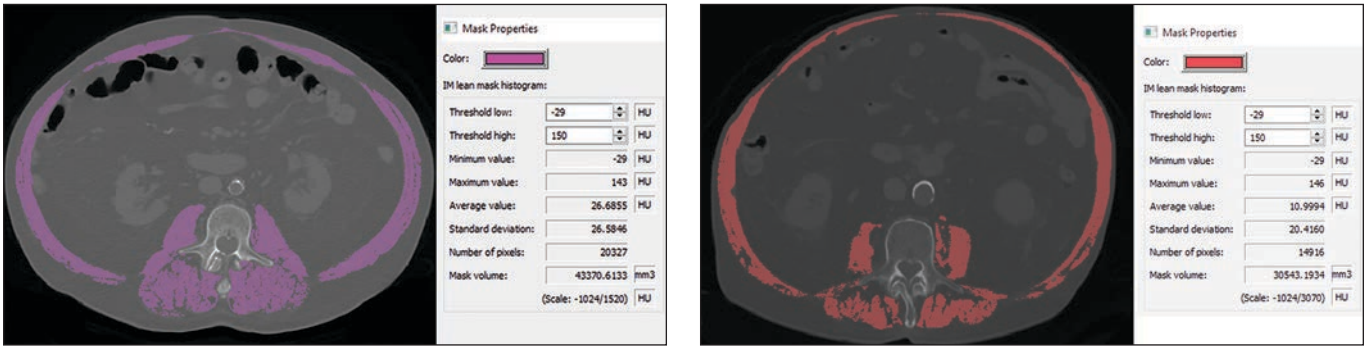

Fig. 5— Images from opportunistic CT of muscle.
A, 67-year-old woman who presented after ground-level fall. Axial CT image obtained at level of L3 shows segmentation of psoas, paraspinous, and abdominal muscles, with threshold of –29 to 150 HU used as shown in mask properties. Muscle cross-sectional area was 86.6 cm^2, and skeletal muscle index was 39.4 cm^2/m^2. Based on skeletal muscle index threshold for women (< 38.5 cm^2/m^2), measurement is within range considered normal.
B, 61-year-old man who presented with flank pain. Axial CT image obtained at level of L3 shows segmentation of psoas, paraspinous, and abdominal muscles, with threshold of –29 to 150 HU used as shown in mask properties. Muscle cross-sectional area was 61.1 cm^2, and skeletal muscle index was 19.7 cm^2/m^2. Based on skeletal muscle index threshold for men (< 52.4 cm^2/m^2), measurement is within range indicating sarcopenia.

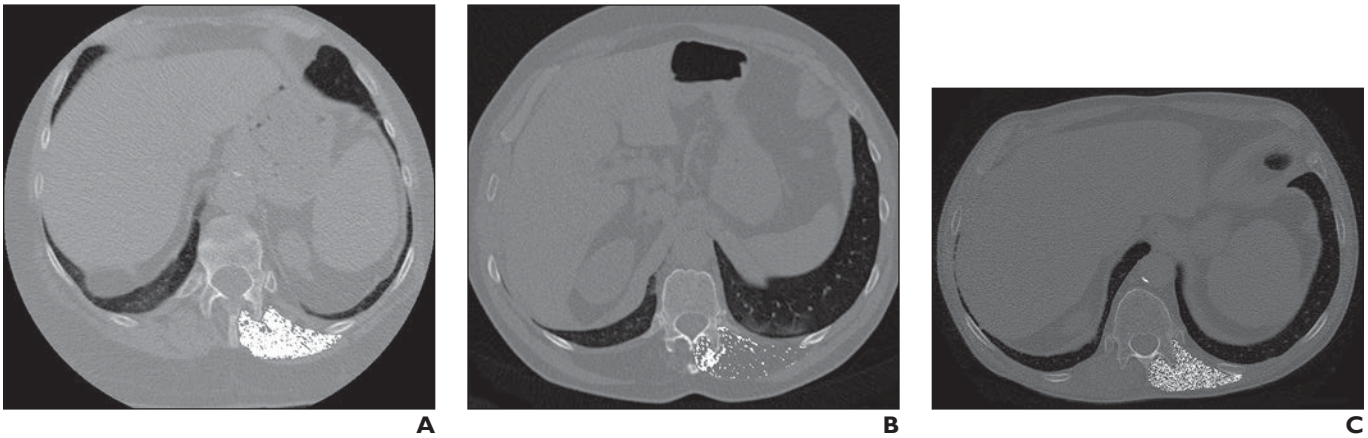

Fig. 6—Images from opportunistic CT of muscle.
A, 72-year-old man who presented for lung cancer screening. Axial CT image obtained at level of T12 shows segmentation of left paraspinous muscles, with use of threshold of –29 to 150 HU. Muscle area and attenuation appear normal.
B, 74-year-old woman who presented for lung cancer screening. Axial CT image obtained at level of T12 shows segmentation of left paraspinous muscles, with use of threshold of –29 to 150 HU. Muscle area and attenuation appear diminished.
C, 71-year-old woman who presented for lung cancer screening. Axial CT image obtained at level of T12 shows segmentation of left paraspinous muscles, with use of threshold of –29 to 150 HU. Muscle cross-sectional area appears normal, whereas muscle attenuation appears diminished.

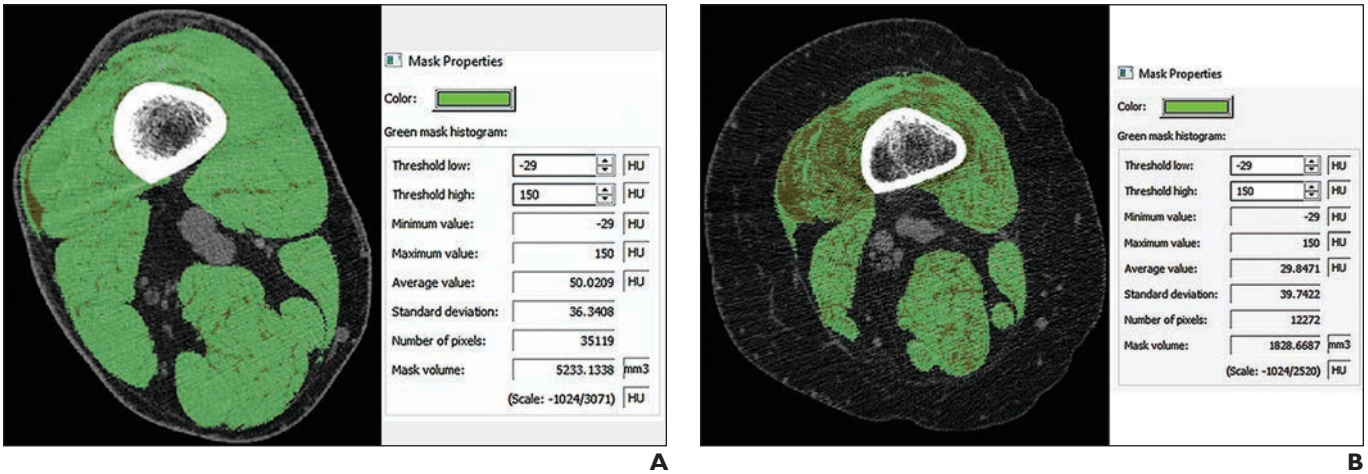

Fig. 7—Images from opportunistic CT of muscle.
A, 60-year-old man who presented for preoperative evaluation for partial knee replacement. Axial CT image obtained at level of distal thigh shows segmentation of thigh muscles, with threshold of –29 to 150 HU used as shown in mask properties. Although there currently is no consensus on diagnostic thresholds for thigh muscle area, muscle area and attenuation subjectively appear to be in range considered normal.
B, 61-year-old woman who presented for preoperative evaluation for partial knee replacement. Axial CT image obtained at level of distal thigh shows segmentation of thigh muscles, with threshold of –29 to 150 HU used as shown in mask properties. Although there currently is no consensus on diagnostic thresholds for thigh muscle area, muscle area and attenuation subjectively appear to be diminished.

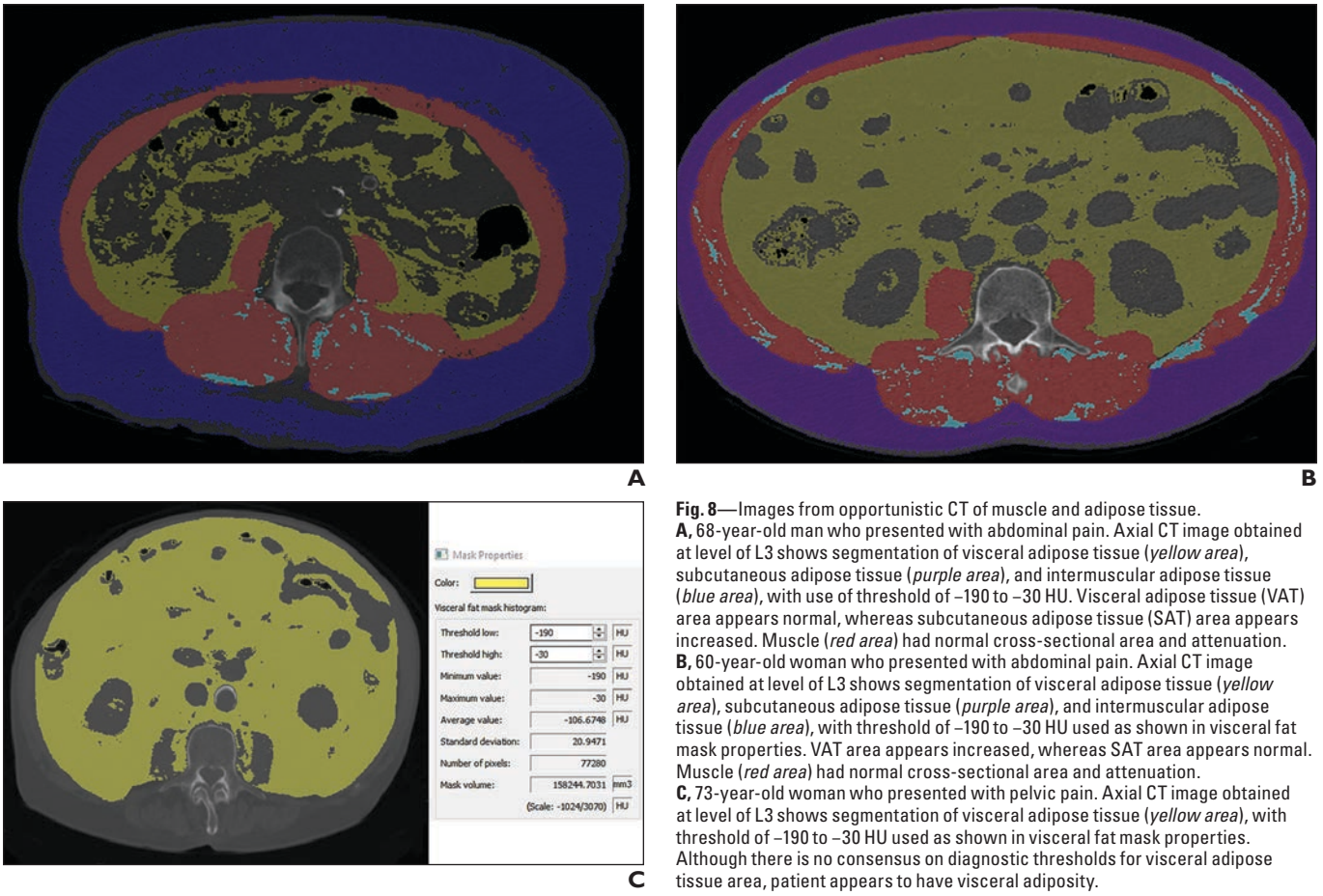

Fig. 8—Images from opportunistic CT of muscle and adipose tissue.
A, 68-year-old man who presented with abdominal pain. Axial CT image obtained at level of L3 shows segmentation of visceral adipose tissue (*yellow area*), subcutaneous adipose tissue (*purple area*), and intermuscular adipose tissue (*blue area*), with use of threshold of –190 to –30 HU. Visceral adipose tissue (VAT) area appears normal, whereas subcutaneous adipose tissue (SAT) area appears increased. Muscle (*red area*) had normal cross-sectional area and attenuation.
B, 60-year-old woman who presented with abdominal pain. Axial CT image obtained at level of L3 shows segmentation of visceral adipose tissue (*yellow area*), subcutaneous adipose tissue (*purple area*), and intermuscular adipose tissue (*blue area*), with threshold of –190 to –30 HU used as shown in visceral fat mask properties. VAT area appears increased, whereas SAT area appears normal. Muscle (*red area*) had normal cross-sectional area and attenuation.
C, 73-year-old woman who presented with pelvic pain. Axial CT image obtained at level of L3 shows segmentation of visceral adipose tissue (*yellow area*), with threshold of –190 to –30 HU used as shown in visceral fat mask properties. Although there is no consensus on diagnostic thresholds for visceral adipose tissue area, patient appears to have visceral adiposity.

CT-derived muscle attenuation is also increasingly assessed as an indicator of muscle fat content. Both a low skeletal muscle index (i.e., myopenia) and low muscle attenuation (i.e., myosteatosis) have been associated with adverse outcomes. Since the publication of a detailed review on sarcopenia in the *AJR* [83], there has been increasing evidence that opportunistic CT assessment of myosteatosis adds prognostic value [93]. In addition to assessment of intermuscular adipose tissue, simultaneous evaluation of other tissues can be performed, including visceral adipose tissue and subcutaneous adipose tissue (Fig. 8).

Opportunistic CT has been extensively validated as a tool to help stratify the risk of adverse clinical outcomes, such as postprocedural complications and death (Appendix 2). Fully automated tools for tissue segmentation and quantification are now used by many researchers funded by the National Institutes of Health [94–96], but access to the computer code for physicians and patients remains limited at this time.

Prevention and Treatment

Recently, two umbrella reviews summarized current evidence for prevention and treatment of sarcopenia using exercise and medications. For exercise interventions relevant to older adults [97], one of the umbrella reviews analyzed 14 systematic reviews (seven with meta-analyses) and focused on four exercise categories: resistance training, resistance training with nutritional supplementation, multimodal exercise programs, and blood flow restriction training. This analysis found high-quality evidence for a positive effect of resistance training on muscle mass, muscle strength, and physical performance. Results showed that high-intensity resistance training is more efficacious than low-intensity resistance training (i.e., 70–80% of maximal effort, rather than ≤ 50% of one maximum repetition). Specific exercise recommendations from this research include the following: train large-muscle groups throughout the body with four sets of eight to 15 repetitions per muscle group (two to three times per week). Of interest, a relatively unknown training method called blood flow restriction training was found to have a significant impact on muscle strength. Nutritional supplementation, however, had limited benefit in these systematic reviews evaluating the prevention and treatment of sarcopenia in elderly populations. For populations with cancer who commonly have muscle depletion (cachexia), however, a recent systematic review [98] concluded that combined exercise and nutritional interventions result in improvements in multiple clinical domains.

In the second umbrella review (of seven systematic reviews or meta-analyses) [99], 10 currently available pharmacologic interventions were evaluated. Only two of 10 agents were found to be useful in improving muscle mass, muscle strength, physical performance, or a combination of these: vitamin D (especially in older women) and testosterone (in older men with clinical muscle weakness and low serum testosterone levels).

Currently, 116 trials (as listed in the ClinicalTrials.gov database) are in progress to evaluate exercise, diet, supplements, and

pharmaceuticals for sarcopenia. Regardless of the cause of muscle depletion (e.g., age-related sarcopenia or cancer-related cachexia), earlier diagnosis using opportunistic CT could allow interventions earlier in the disease course when the window of anabolic potential is open [100].

Conclusion

Osteoporosis and sarcopenia are increasingly common in older adults, and the resulting impact on adverse health outcomes is immense. Osteoporosis is currently underdiagnosed and undertreated, even though there are efficacious treatments. Osteoporosis is associated with fragility fractures, and some of these fractures are associated with reduced survival. Osteoporosis is also associated with postoperative hardware complications, but these complications may be minimized by selecting appropriate implants. Sarcopenia, identified on CT as low muscle mass and attenuation, is associated with morbidity and mortality. CT-derived thresholds for diagnosing low muscle mass and attenuation have been established in several large studies, and best practices for sarcopenia diagnosis, prevention, and treatment are emerging. With opportunistic CT, we now have the opportunity to add further value to routine imaging with biomarkers that assess bone and muscle health without additional examination time or radiation.

References

1. U.S. Census Bureau. Historical estimates of world population. U.S. Census Bureau website. www.census.gov/data/tables/time-series/demo/international-programs/historical-est-worldpop.html. Accessed June 7, 2020
2. Riley JC. Estimates of regional and global life expectancy, 1800–2001. *Popul Dev Rev* 2005; 31:537–543
3. World Health Organization (WHO). World health statistics 2020 visual summary. WHO website. www.who.int/data/gho/whs-2020-visual-summary. Accessed June 7, 2020
4. United Nations (UN). World population prospects 2019. UN website. population.un.org/wpp/Graphs//DemographicProfiles/Line/900. Accessed June 7, 2020
5. Centers for Medicare & Medicaid Services (CMS). National health expenditure projections 2018–2027: forecast summary. CMS website. www.cms.gov/Research-Statistics-Data-and-Systems/Statistics-Trends-and-Reports/NationalHealthExpendData/Downloads/ForecastSummary.pdf. Published February 20, 2019. Accessed January 1, 2020
6. Papanicolas I, Woskie LR, Jha AK. Health care spending in the United States and other high-income countries. *JAMA* 2018; 319:1024–1039
7. Smith-Bindman R, Miglioretti DL, Johnson E, et al. Use of diagnostic imaging studies and associated radiation exposure for patients enrolled in large integrated health care systems, 1996-2010. *JAMA* 2012; 307:2400–2409
8. Oren O, Kebebew E, Ioannidis JPA. Curbing unnecessary and wasted diagnostic imaging. *JAMA* 2019; 321:245–246
9. Kosse C, Lane E. Medicare's new rules seek to expand price transparency: what this—and other regulatory proposals—mean for imaging. Advisory Board website. www.advisory.com/research/imaging-performance-partnership/the-reading-room/2019/08/price-transparency. Published August 20, 2019. Accessed January 1, 2020
10. Organisation for Economic Co-operation and Development (OECD). Health care resources. OECD website. stats.oecd.org/index.aspx?queryid=30184. Accessed January 1, 2020
11. Radwan RW, Tang AM, Beasley WD. Computed tomography as a first-line investigation for elderly patients admitted to a surgical assessment unit. *Ann R Coll Surg Engl* 2018; 100:285–289
12. Lenchik L, Lenoir KM, Tan J, et al. Opportunistic measurement of skeletal muscle size and muscle attenuation on computed tomography predicts 1-year mortality in Medicare patients. *J Gerontol A Biol Sci Med Sci* 2019; 74:1063–1069
13. Boutin RD, Bamrungchart S, Bateni CP, et al. CT of patients with hip fracture: muscle size and attenuation help predict mortality. *AJR* 2017; 208:[web]W208–W215
14. O'Connor SD, Graffy PM, Zea R, Pickhardt PJ. Does nonenhanced CT-based quantification of abdominal aortic calcification outperform the Framingham Risk Score in predicting cardiovascular events in asymptomatic adults? *Radiology* 2019; 290:108–115
15. Graffy PM, Liu J, O'Connor S, Summers RM, Pickhardt PJ. Automated segmentation and quantification of aortic calcification at abdominal CT: application of a deep learning-based algorithm to a longitudinal screening cohort. *Abdom Radiol (NY)* 2019; 44:2921–2928
16. Lee SJ, Liu J, Yao J, Kanarek A, Summers RM, Pickhardt PJ. Fully automated segmentation and quantification of visceral and subcutaneous fat at abdominal CT: application to a longitudinal adult screening cohort. *Br J Radiol* 2018; 91:20170968
17. Graffy PM, Sandfort V, Summers RM, Pickhardt PJ. Automated liver fat quantification at nonenhanced abdominal CT for population-based steatosis assessment. *Radiology* 2019; 293:334–342
18. Pickhardt PJ, Malecki K, Hunt OF, et al. Hepatosplenic volumetric assessment at MDCT for staging liver fibrosis. *Eur Radiol* 2017; 27:3060–3068
19. Amini B, Boyle SP, Boutin RD, Lenchik L. Approaches to assessment of muscle mass and myosteatosis on computed tomography: a systematic review. *J Gerontol A Biol Sci Med Sci* 2019; 74:1671–1678
20. Boutin RD, Kaptuch JM, Bateni CP, Chalfant JS, Yao L. Influence of IV contrast administration on CT measures of muscle and bone attenuation: implications for sarcopenia and osteoporosis evaluation. *AJR* 2016; 207:1046–1054
21. Szczykutowicz TP, DuPlissis A, Pickhardt PJ. Variation in CT number and image noise uniformity according to patient positioning in MDCT. *AJR* 2017; 208:1064–1072
22. Li K, Tang J, Chen GH. Statistical model based iterative reconstruction (MBIR) in clinical CT systems: experimental assessment of noise performance. *Med Phys* 2014; 41:041906
23. Mileto A, Barina A, Marin D, et al. Virtual monochromatic images from dual-energy multidetector CT: variance in CT numbers from the same lesion between single-source projection-based and dual-source image-based implementations. *Radiology* 2016; 279:269–277
24. Fuchs G, Chretien YR, Mario J, et al. Quantifying the effect of slice thickness, intravenous contrast and tube current on muscle segmentation: implications for body composition analysis. *Eur Radiol* 2018; 28:2455–2463
25. Morsbach F, Zhang YH, Martin L, Lindqvist C, Brismar T. Body composition evaluation with computed tomography: contrast media and slice thickness cause methodological errors. *Nutrition* 2019; 59:50–55
26. Lamba R, McGahan JP, Corwin MT, et al. CT Hounsfield numbers of soft tissues on unenhanced abdominal CT scans: variability between two different manufacturers' MDCT scanners. *AJR* 2014; 203:1013–1020
27. Engelke K. Quantitative computed tomography: current status and new developments. *J Clin Densitom* 2017; 20:309–321
28. Engelke K, Museyko O, Wang L, Laredo JD. Quantitative analysis of skeletal muscle by computed tomography imaging: state of the art. *J Orthop Translat* 2018; 15:91–103
29. Bae KT. Intravenous contrast medium administration and scan timing at CT: considerations and approaches. *Radiology* 2010; 256:32–61
30. Pompe E, Willemink MJ, Dijkhuis GR, Verhaar HJ, Mohamed Hoesein FA, de Jong PA. Intravenous contrast injection significantly affects bone mineral density measured on CT. *Eur Radiol* 2015; 25:283–289
31. Pickhardt PJ, Lauder T, Pooler BD, et al. Effect of IV contrast on lumbar trabecular attenuation at routine abdominal CT: correlation with DXA

and implications for opportunistic osteoporosis screening. *Osteoporos Int* 2016; 27:147–152

32. Link TM, Koppers BB, Licht T, Bauer J, Lu Y, Rummeny EJ. In vitro and in vivo spiral CT to determine bone mineral density: initial experience in patients at risk for osteoporosis. *Radiology* 2004; 231:805–811
33. Bauer JS, Henning TD, Müeller D, Lu Y, Majumdar S, Link TM. Volumetric quantitative CT of the spine and hip derived from contrast-enhanced MDCT: conversion factors. *AJR* 2007; 188:1294–1301
34. van Vugt JLA, Coebergh van den Braak RRJ, Schippers HJW, et al. Contrast-enhancement influences skeletal muscle density, but not skeletal muscle mass, measurements on computed tomography. *Clin Nutr* 2018; 37:1707–1714
35. van der Werf A, Dekker IM, Meijerink MR, Wierdsma NJ, de van der Schueren MAE, Langius JAE. Skeletal muscle analyses: agreement between non-contrast and contrast CT scan measurements of skeletal muscle area and mean muscle attenuation. *Clin Physiol Funct Imaging* 2018; 38:366–372
36. Garner HW, Paturzo MM, Gaudier G, Pickhardt PJ, Wessell DE. Variation in attenuation in L1 trabecular bone at different tube voltages: caution is warranted when screening for osteoporosis with the use of opportunistic CT. *AJR* 2017; 208:165–170
37. Schwaiger BJ, Gersing AS, Baum T, Noël PB, Zimmer C, Bauer JS. Bone mineral density values derived from routine lumbar spine multidetector row CT predict osteoporotic vertebral fractures and screw loosening. *AJNR* 2014; 35:1628–1633
38. Morsbach F, Zhang YH, Nowik P, et al. Influence of tube potential on CT body composition analysis. *Nutrition* 2018; 53:9–13
39. Rollins KE, Awwad A, Macdonald IA, Lobo DN. A comparison of two different software packages for analysis of body composition using computed tomography images. *Nutrition* 2019; 57:92–96
40. van Vugt JL, Levolger S, Gharbharan A, et al. A comparative study of software programmes for cross-sectional skeletal muscle and adipose tissue measurements on abdominal computed tomography scans of rectal cancer patients. *J Cachexia Sarcopenia Muscle* 2017; 8:285–297
41. Barbalho ER, Rocha IMGD, Medeiros GOC, Friedman R, Fayh APT. Agreement between software programmes of body composition analyses on abdominal computed tomography scans of obese adults. *Arch Endocrinol Metab* 2019; 64:24–29 [Epub ahead of print]
42. Pompe E, de Jong PA, de Jong WU, et al. Inter-observer and inter-examination variability of manual vertebral bone attenuation measurements on computed tomography. *Eur Radiol* 2016; 26:3046–3053
43. Jang S, Graffy PM, Ziemlewicz TJ, Lee SJ, Summers RM, Pickhardt PJ. Opportunistic osteoporosis screening at routine abdominal and thoracic CT: normative L1 trabecular attenuation values in more than 20,000 adults. *Radiology* 2019; 291:360–367
44. Barnard R, Tan J, Roller B, et al. Machine learning for automatic paraspinous muscle area and attenuation measures on low-dose chest CT scans. *Acad Radiol* 2019; 26:1686–1694
45. Lenchik L, Heacock L, Weaver AA, et al. Automated segmentation of tissues using CT and MRI: a systematic review. *Acad Radiol* 2019; 26:1695–1706
46. Kullberg J, Hedström A, Brandberg J, et al. Automated analysis of liver fat, muscle and adipose tissue distribution from CT suitable for large-scale studies. *Sci Rep* 2017; 7:10425
47. Cortet B. Does low bone mineral density predict mortality? *Joint Bone Spine* 2016; 83:623–624
48. Lewiecki EM, Ortendahl JD, Vanderpuye-Orgle J, et al. Healthcare policy changes in osteoporosis can improve outcomes and reduce costs in the United States. *JBMR Plus* 2019; 3:e10192
49. des Bordes J, Prasad S, Pratt G, Suarez-Almazor ME, Lopez-Olivo MA. Knowledge, beliefs, and concerns about bone health from a systematic review and metasynthesis of qualitative studies. *PLoS One* 2020; 15:e0227765
50. Merle B, Haesebaert J, Bedouet A, et al. Osteoporosis prevention: where are the barriers to improvement in French general practitioners? A qualitative study. *PLoS One* 2019; 14:e0219681
51. Merlijn T, Swart KMA, van der Horst HE, Netelenbos JC, Elders PJM. Fracture prevention by screening for high fracture risk: a systematic review and meta-analysis. *Osteoporos Int* 2019; 31:251–257 [Epub ahead of print]
52. Overman RA, Farley JF, Curtis JR, Zhang J, Gourlay ML, Deal CL. DXA utilization between 2006 and 2012 in commercially insured younger postmenopausal women. *J Clin Densitom* 2015; 18:145–149
53. Barton DW, Behrend CJ, Carmouche JJ. Rates of osteoporosis screening and treatment following vertebral fracture. *Spine J* 2019; 19:411–417
54. Malik AT, Retchin S, Phillips FM, et al. Declining trend in osteoporosis management and screening following vertebral compression fractures: a national analysis of commercial insurance and medicare advantage beneficiaries. *Spine J* 2019; 20:538–546
55. Link TM, Lang TF. Axial QCT: clinical applications and new developments. *J Clin Densitom* 2014; 17:438–448
56. Ziemlewicz TJ, Maciejewski A, Binkley N, Brett AD, Brown JK, Pickhardt PJ. Direct comparison of unenhanced and contrast-enhanced CT for opportunistic proximal femur bone mineral density measurement: implications for osteoporosis screening. *AJR* 2016; 206:694–698
57. Lee SJ, Binkley N, Lubner MG, Bruce RJ, Ziemlewicz TJ, Pickhardt PJ. Opportunistic screening for osteoporosis using the sagittal reconstruction from routine abdominal CT for combined assessment of vertebral fractures and density. *Osteoporos Int* 2016; 27:1131–1136
58. Lee SJ, Pickhardt PJ. Opportunistic screening for osteoporosis using body CT scans obtained for other indications: the UW experience. *Clin Rev Bone Miner Metab* 2017; 15:128–137
59. Pickhardt PJ, Lee LJ, del Rio AM, et al. Simultaneous screening for osteoporosis at CT colonography: bone mineral density assessment using MDCT attenuation techniques compared with the DXA reference standard. *J Bone Miner Res* 2011; 26:2194–2203
60. Graffy PM, Lee SJ, Ziemlewicz TJ, Pickhardt PJ. Prevalence of vertebral compression fractures on routine CT scans according to L1 trabecular attenuation: determining relevant thresholds for opportunistic osteoporosis screening. *AJR* 2017; 209:491–496
61. Lee SJ, Graffy PM, Zea RD, Ziemlewicz TJ, Pickhardt PJ. Future osteoporotic fracture risk related to lumbar vertebral trabecular attenuation measured at routine body CT. *J Bone Miner Res* 2018; 33:860–867
62. Urrutia J, Besa P, Piza C. Incidental identification of vertebral compression fractures in patients over 60 years old using computed tomography scans showing the entire thoraco-lumbar spine. *Arch Orthop Trauma Surg* 2019; 139:1497–1503
63. Löffler MT, Jacob A, Valentinitsch A, et al. Improved prediction of incident vertebral fractures using opportunistic QCT compared to DXA. *Eur Radiol* 2019; 29:4980–4989
64. Bredow J, Boese CK, Werner CM, et al. Predictive validity of preoperative CT scans and the risk of pedicle screw loosening in spinal surgery. *Arch Orthop Trauma Surg* 2016; 136:1063–1067
65. Mi J, Li K, Zhao X, Zhao CQ, Li H, Zhao J. Vertebral body Hounsfield units are associated with cage subsidence after transforaminal lumbar interbody fusion with unilateral pedicle screw fixation. *Clin Spine Surg* 2017; 30:E1130–E1136
66. Schreiber JJ, Hughes AP, Taher F, Girardi FP. An association can be found between hounsfield units and success of lumbar spine fusion. *HSS J* 2014; 10:25–29
67. Meredith DS, Schreiber JJ, Taher F, Cammisa FP Jr, Girardi FP. Lower preoperative Hounsfield unit measurements are associated with adjacent segment fracture after spinal fusion. *Spine* 2013; 38:415–418
68. Zaidi Q, Danisa OA, Cheng W. Measurement techniques and utility of Hounsfield unit values

for assessment of bone quality prior to spinal instrumentation: a review of current literature. *Spine* 2019; 44:E239–E244

69. Anderson PA, Polly DW, Binkley NC, Pickhardt PJ. Clinical use of opportunistic computed tomography screening for osteoporosis. *J Bone Joint Surg Am* 2018; 100:2073–2081
70. Buerba RA, Sharma A, Ziino C, Arzeno A, Ajiboye RM. Bisphosphonate and teriparatide use in thoracolumbar spinal fusion: a systematic review and meta-analysis of comparative studies. *Spine* 2018; 43:E1014–E1023
71. Ji C, Yu S, Yan N, et al. Risk factors for subsidence of titanium mesh cage following single-level anterior cervical corpectomy and fusion. *BMC Musculoskelet Disord* 2020; 21:32
72. Therkildsen J, Winther S, Nissen L, et al. Feasibility of opportunistic screening for low thoracic bone mineral density in patients referred for routine cardiac CT. *J Clin Densitom* 2018 Dec 17 [Epub ahead of print]
73. Na MK, Won YD, Kim CH, et al. Opportunistic osteoporosis screening via the measurement of frontal skull Hounsfield units derived from brain computed tomography images. *PLoS One* 2018; 13:e0197336
74. Pervaiz K, Cabezas A, Downes K, Santoni BG, Frankle MA. Osteoporosis and shoulder osteoarthritis: incidence, risk factors, and surgical implications. *J Shoulder Elbow Surg* 2013; 22:e1–e8
75. Schreiber JJ, Gausden EB, Anderson PA, Carlson MG, Weiland AJ. Opportunistic osteoporosis screening: gleaning additional information from diagnostic wrist CT scans. *J Bone Joint Surg Am* 2015; 97:1095–1100
76. Hoel RJ, Ledonio CG, Takahashi T, Polly DW Jr. Sacral bone mineral density (BMD) assessment using opportunistic CT scans. *J Orthop Res* 2017; 35:160–166
77. Donohue D, Decker S, Ford J, et al. Opportunistic CT screening for osteoporosis in patients with pelvic and acetabular trauma: technique and potential clinical impact. *J Orthop Trauma* 2018; 32:408–413
78. Lee SY, Kwon SS, Kim HS, et al. Reliability and validity of lower extremity computed tomography as a screening tool for osteoporosis. *Osteoporos Int* 2015; 26:1387–1394
79. Tie K, Wang H, Wang X, Chen L. Measurement of bone mineral density in the tunnel regions for anterior cruciate ligament reconstruction by dual-energy x-ray absorptiometry, computed tomography scan, and the immersion technique based on Archimedes' principle. *Arthroscopy* 2012; 28:1464–1471
80. Panchbhavi VK, Boutris N, Patel K, Molina D, Andersen CR. CT density analysis of the medial cuneiform. *Foot Ankle Int* 2013; 34:1596–1599
81. Hollensteiner M, Sandriesser S, Bliven E, von Rüden C, Augat P. Biomechanics of osteoporotic fracture fixation. *Curr Osteoporos Rep* 2019; 17:363–374
82. Cruz-Jentoft AJ, Bahat G, Bauer J, et al.; Writing Group for the European Working Group on Sarcopenia in Older People 2 (EWGSOP2), and the Extended Group for EWGSOP2. Sarcopenia: revised European consensus on definition and diagnosis. *Age Ageing* 2019; 48:16–31
83. Boutin RD, Yao L, Canter RJ, Lenchik L. Sarcopenia: current concepts and imaging implications. *AJR* 2015; 205:W255–W266
84. Cawthon PM, Travison TG, Manini TM, et al.; Sarcopenia Definition and Outcomes Consortium Conference Participants. Establishing the link between lean mass and grip strength cutpoints with mobility disability and other health outcomes: Proceedings of the Sarcopenia Definition and Outcomes Consortium Conference. *J Gerontol A Biol Sci Med Sci* 2019 Mar 14 [Epub ahead of print]
85. Kotlarczyk MP, Perera S, Nace DA, Resnick NM, Greenspan SL. Identifying sarcopenia in female long-term care residents: a comparison of current guidelines. *J Am Geriatr Soc* 2018; 66:316–320
86. Kemmler W, Teschler M, Weißenfels A, Sieber C, Freiberger E, von Stengel S. Prevalence of sarcopenia and sarcopenic obesity in older German men using recognized definitions: high accordance but low overlap! *Osteoporos Int* 2017; 28:1881–1891
87. Bianchi L, Maietti E, Abete P, et al. GLISTEN Group Investigators. Comparing EWGSOP2 and FNIH sarcopenia definitions: agreement and three-year survival prognostic value in older hospitalized adults. The GLISTEN Study. *J Gerontol A Biol Sci Med Sci* 2019 Oct 19 [Epub ahead of print]
88. Reiss J, Iglseder B, Alzner R, et al. Consequences of applying the new EWGSOP2 guideline instead of the former EWGSOP guideline for sarcopenia case finding in older patients. *Age Ageing* 2019; 48:719–724
89. Papadopoulou SK, Tsintavis P, Potsaki P, Papandreou D. Differences in the prevalence of sarcopenia in community-dwelling, nursing home and hospitalized individuals: a systematic review and meta-analysis *J Nutr Health Aging* 2020; 24:83–90
90. Pacifico J, Geerlings MAJ, Reijnierse EM, Phassouliotis C, Lim WK, Maier AB. Prevalence of sarcopenia as a comorbid disease: a systematic review and meta-analysis. *Exp Gerontol* 2020 Oct 19 [Epub ahead of print]
91. Peng TC, Chen WL, Wu LW, Chang YW, Kao TW. Sarcopenia and cognitive impairment: a systematic review and meta-analysis. *Clin Nutr* 2019 Dec 17 [Epub ahead of print]
92. Hopkins JJ, Skubleny D, Bigam DL, Baracos VE, Eurich DT, Sawyer MB. Barriers to the interpretation of body composition in colorectal cancer: a review of the methodological inconsistency and complexity of the CT-defined body habitus. *Ann Surg Oncol* 2018; 25:1381–1394
93. Martin L, Gioulbasanis I, Senesse P, Baracos VE. Cancer-associated malnutrition and CT-defined sarcopenia and myosteatosis are endemic in overweight and obese patients. *JPEN J Parenter Enteral Nutr* 2019; 44: [Epub ahead of print]
94. Graffy PM, Liu J, Pickhardt PJ, Burns JE, Yao J, Summers RM. Deep learning-based muscle segmentation and quantification at abdominal CT: application to a longitudinal adult screening cohort for sarcopenia assessment. *Br J Radiol* 2019; 92:20190327
95. Burns JE, Yao J, Chalhoub D, Chen JJ, Summers RM. A machine learning algorithm to estimate sarcopenia on abdominal CT. *Acad Radiol* 2020; 27:311–320
96. Hemke R, Buckless CG, Tsao A, Wang B, Torriani M. Deep learning for automated segmentation of pelvic muscles, fat, and bone from CT studies for body composition assessment. *Skeletal Radiol* 2020; 49:387–395
97. Beckwée D, Delaere A, Aelbrecht S, et al. Exercise interventions for the prevention and treatment of sarcopenia: a systematic umbrella review. *J Nutr Health Aging* 2019; 23:494–502
98. Hall CC, Cook J, Maddocks M, Skipworth RJE, Fallon M, Laird BJ. Combined exercise and nutritional rehabilitation in outpatients with incurable cancer: a systematic review. *Support Care Cancer* 2019; 27:2371–2384
99. De Spiegeleer A, Beckwée D, Bautmans I, Petrovic M; Sarcopenia Guidelines Development group of the Belgian Society of Gerontology and Geriatrics (BSGG). Pharmacological interventions to improve muscle mass, muscle strength and physical performance in older people: an umbrella review of systematic reviews and meta-analyses. *Drugs Aging* 2018; 35:719–734
100. Prado CM, Purcell SA, Laviano A. Nutrition interventions to treat low muscle mass in cancer. *J Cachexia Sarcopenia Muscle* 2020; 11:366–380
101. Pickhardt PJ, Pooler BD, Lauder T, del Rio AM, Bruce RJ, Binkley N. Opportunistic screening for osteoporosis using abdominal computed tomography scans obtained for other indications. *Ann Intern Med* 2013; 158:588–595
102. Buckens CF, Dijkhuis G, de Keizer B, Verhaar HJ, de Jong PA. Opportunistic screening for osteoporosis on routine computed tomography? An external validation study. *Eur Radiol* 2015; 25:2074–2079
103. Alacreu E, Moratal D, Arana E. Opportunistic screening for osteoporosis by routine CT in South-

ern Europe. *Osteoporos Int* 2017; 28:983–990

104. Gausden EB, Nwachukwu BU, Schreiber JJ, Lorich DG, Lane JM. Opportunistic use of CT imaging for osteoporosis screening and bone density assessment: a qualitative systematic review. *J Bone Joint Surg Am* 2017; 99:1580–1590
105. Pickhardt PJ, Lee SJ, Liu J, et al. Population-based opportunistic osteoporosis screening: Validation of a fully automated CT tool for assessing longitudinal BMD changes. *Br J Radiol* 2019; 92:20180726
106. Borggreve AS, den Boer RB, van Boxel GI, et al. The predictive value of low muscle mass as measured on CT scans for postoperative complications and mortality in gastric cancer patients: a systematic review and meta-analysis. *J Clin Med* 2020; 9:E199
107. Rinninella E, Cintoni M, Raoul P, et al. Muscle mass, assessed at diagnosis by L3-CT scan as a prognostic marker of clinical outcomes in patients with gastric cancer: a systematic review and meta-analysis. *Clin Nutr* 2019 Nov 1 [Epub ahead of print]
108. Nishimura JM, Ansari AZ, D'Souza DM, Moffatt-Bruce SD, Merritt RE, Kneuertz PJ. Computed tomography-assessed skeletal muscle mass as a predictor of outcomes in lung cancer surgery. *Ann Thorac Surg* 2019; 108:1555–1564
109. Su H, Ruan J, Chen T, Lin E, Shi L. CT-assessed sarcopenia is a predictive factor for both long-term and short-term outcomes in gastrointestinal oncology patients: a systematic review and meta-analysis. *Cancer Imaging* 2019; 19:82
110. Cao Q, Xiong Y, Zhong Z, Ye Q. Computed tomography-assessed sarcopenia indexes predict major complications following surgery for hepatopancreatobiliary malignancy: a meta-analysis. *Ann Nutr Metab* 2019; 74:24–34
111. Xia W, Barazanchi AWH, MacFater WS, Hill AG. The impact of computed tomography-assessed sarcopenia on outcomes for trauma patients: a systematic review and meta-analysis. *Injury* 2019; 50:1565–1576
112. Soud M, Alahdab F, Ho G, et al. Usefulness of skeletal muscle area detected by computed tomography to predict mortality in patients undergoing transcatheter aortic valve replacement: a meta-analysis study. *Int J Cardiovasc Imaging* 2019; 35:1141–1147
113. Hu X, Dou WC, Shao YX, et al. The prognostic value of sarcopenia in patients with surgically treated urothelial carcinoma: a systematic review and meta-analysis. *Eur J Surg Oncol* 2019; 45:747–754
114. Shachar SS, Williams GR, Muss HB, Nishijima TF. Prognostic value of sarcopenia in adults with solid tumours: a meta-analysis and systematic review. *Eur J Cancer* 2016; 57:58–67
115. van Vugt JL, Levolger S, de Bruin RW, van Rosmalen J, Metselaar HJ, IJzermans JN. Systematic review and meta-analysis of the impact of computed tomography-assessed skeletal muscle mass on outcome in patients awaiting or undergoing liver transplantation. *Am J Transplant* 2016; 16:2277–2292

APPENDIX 1: Representative Studies (Systematic Reviews and Clinical Trials) of the Use of Opportunistic CT for Osteoporosis Screening in More Than 300 Patients

Study Authors [Reference] (Publication Year)	No. of Patients	CT Parameter(s)	Cut Point	Key Finding(s)	Comment(s)
Pickhardt et al. [101] (2013)	1867	Without and with contrast medium Tube potential not specified	L1 attenuation ≤ 135 HU for osteoporosis (sensitivity, 76%; specificity, 75%)	Routine abdominal CT can be used for osteoporosis screening (without additional imaging, radiation exposure, cost, equipment, or patient time)	CT correlated with DEXA
Buckens et al. [102] (2015)	302	Contrast medium and tube potential not specified	L1 attenuation ≤ 99 HU for osteoporosis (sensitivity, 62%; specificity, 79%)	Validated vertebral trabecular bone attenuation for osteoporosis screening	CT correlated with DEXA
Lee et al. [57] (2016)	571	With contrast medium 120 kV	L1 attenuation ≤ 110 HU for osteoporosis (sensitivity, 52%; specificity, 90%)	Sagittal image can be used both to measure bone attenuation and to detect compression fractures	Attenuation measurements on axial images were slightly lower than those on sagittal images (mean, 7 HU [6%])
Alacreu et al. [103] (2017)	326	94% with contrast medium 120 kV	L1 attenuation ≤ 116 HU for osteoporosis (sensitivity, 60%; specificity, 60%)	L1 attenuation < 60 HU (very low) warrants further evaluation or treatment L1 attenuation > 170 HU (high) excludes osteoporosis	CT correlated with DEXA
Gausden et al. [104] (2017)	9109	Reporting inconsistent	Correlation coefficients ranged from 0.40 to 0.89	Direct measurement of attenuation for osteoporosis screening is not ready for clinical implementation	Systematic review of 37 studies (10 with DEXA correlation)
Graffy et al. [60] (2017)	1966	Without and with contrast medium 120 kV	L1 attenuation ≤ 90 HU for risk of spine fracture (sensitivity, 87%; specificity, 84%)	Odds ratio of 32 for moderate or severe compression fracture with L1 attenuation ≤ 90 HU Fracture prevalence of 49% with L1 attenuation ≤ 50 HU	As L1 attenuation decreased, the vertebral fracture prevalence progressively increased

(Appendix 1 continues on next page)

APPENDIX 1: Representative Studies (Systematic Reviews and Clinical Trials) of the Use of Opportunistic CT for Osteoporosis Screening in More Than 300 Patients (continued)

Study Authors [Reference] (Publication Year)	No. of Patients	CT Parameter(s)	Cut Point	Key Finding(s)	Comment(s)
Lee et al. [61] (2018)	1966	Without and with contrast medium 120 kV	L1 attenuation ≤ 90 HU for risk of any fragility fracture	Low attenuation value associated with risk of future fractures, including in the spine, pelvis, hip, and radius	With increased fracture risk, DEXA was recommended for appropriate treatment follow-up
Pickhardt et al. [105] (2019)	1603	Without contrast medium 120 kV	NA	Fully automated BMD tool can be used for prospective clinical or retrospective population-based evaluation, including longitudinal changes	Unlike DEXA, CT can assess trabecular bone without confounding caused by degenerative changes or cortical bone
Jang et al. [43] (2019)	20,374	Without and with contrast medium 120 kV	NA	L1 attenuation is similar between men and postmenopausal women Mean age-related bone loss of 2.5 HU per y	Mean L1 attenuation was 226 HU for patients < 30 y vs 89 HU for patients ≥ 90 y

Note—NA = not applicable, DEXA = dual-energy x-ray absorptiometry, BMD = bone mineral density.

APPENDIX 2: Representative Systematic Reviews Performed With Meta-Analysis of Evaluation of Sarcopenia With Opportunistic CT

Study Authors [Reference] (Publication Year)	No. of Patients	No. of Studies Reviewed	Clinical Characteristic of Cohort	Key Findings	Comments
Borggreve et al. [106] (2020)	4887	15	Gastric malignancy	Low muscle mass associated with postoperative complications (OR, 2.1) and overall mortality (HR, 1.8)	No consensus on cutpoint definitions of low muscle mass
Rinninella et al. [107] (2019)	5610	20	Gastric malignancy	Low muscle mass associated with longer hospitalization, postoperative complications (OR, 1.8), and poorer OS (HR, 2.0)	Prevalence of 33%
Nishimura et al. [108] (2019)	1010	9	Lung malignancy surgery	Sarcopenia associated with higher risk of perioperative complications (OR, 2.5) and worse survival (HR, 2.3)	Wide variation in prevalence of sarcopenia (22–56%)
Su et al. [109] (2019)	21,875	70	Gastrointestinal malignancy	Preoperative sarcopenia is associated with major complications (RR, 1.2) and overall mortality (HR, 1.6) and is a risk factor for adverse long-term and short-term outcomes	Prevalence of sarcopenia depends mostly on choice of diagnostic cutpoints
Cao et a [110] (2019)	6656	28	Hepatopancreatobiliary malignancy surgery	Major postoperative complications were associated with SMI (RR, 1.4), psoas muscle index (RR, 1.4), muscle attenuation (RR, 1.4), and intramuscular adipose tissue (RR, 1.6)	No consensus on cutpoint definitions of low muscle mass and quality
Xia et al. [111] (2019)	2867	10	Trauma	Sarcopenia associated with death during inpatient stay (RR, 2.0) and at 30 days (RR, 1.6) and 1 year (RR, 3.1) after inpatient stay	Wide variation in prevalence of sarcopenia (25–71%)
Soud et al. [112] (2019)	1881	8	Transcatheter aortic valve replacement	Higher SMA associated with lower long-term mortality rate (OR, 0.5)	May help to identify high-risk patients for therapy before and after procedure
Hu et al. [113] (2019)	2075	12	Urothelial carcinoma	Sarcopenia associated with worse OS (HR, 1.9) and cancer-specific survival (HR, 2.0)	NA
Shachar et al. [114] (2016)	7843	38	Malignancy (solid tumors)	Sarcopenia associated with poor OS (HR, 1.4) and cancer-specific survival (HR, 1.9)	NA
van Vugt et al. [115] (2016)	3803	19	Liver transplant	Sarcopenia associated with death (HR, 1.8)	Wide variation in prevalence of sarcopenia (22–70%)

Note—OR = odds ratio, HR = hazard ratio, OS = overall survival, RR = risk ratio, SMI = skeletal muscle index, SMA = skeletal muscle area, NA = not applicable.